Pixel-Level Image Fusion using Kalman Algorithm

S. A. Quadri and Othman Sidek

Collaborative µ-electronic Design Excellence Centre (CEDEC)
Engineering Campus, Universiti Sains Malaysia (USM), Penang, Malaysia
reachquadri@yahoo.com

Abstract

Data fusion aims at synergistic use of information and knowledge from different sources to aid in the overall understanding of a phenomenon. In the domain of remote sensing, where images are acquired by multiple sources or by the same source in multiple acquisition contexts, the data made available by different sources are complementary to each other, proper fusion of the data can bring better and consistent interpretation of the scene. The paper presents application of Kalman filter at pixel-level fusion. The input data collected from Ozone Monitoring Instrument (OMI) on NASA's Aura satellite is subjected to the proposed algorithm. The performance of the algorithm is evaluated by few well-known image quality metrics.

Keywords: *Data Fusion, Satellite data, Image quality metrics, Kalman filter*

1. Introduction

The course of action to combine multiple frames of the same scene into one image is known as image fusion. It is a procedure to acquire complete information representation of the same scene, such as temporal, spectral and spatial information for better understanding and inferences. It can improve the robustness of the multi-sensor system to the variation of condition and occasion, and it can reject or filter some uncorrelated or redundant information. Due to the predictable benefits of multi-sensor image fusion, the applications of image fusion have been successfully extended to remote sensing applications [1].

Although, Kalman filter was designed for optimal control of navigation, because of its inherent potential it has been used for various engineering applications including real-time imaging [2]. The Kalman filtering algorithm [3] works by combining the information regarding the system dynamics with probabilistic information regarding the noise. The filter is very prevailing in that it supports estimations of past, present and even future states and, in particular, can do so even when the precise nature of the noise is unknown. In addition to the basic mechanism of the filter to reduce the noise, the algorithm provides a running average of fusion of pixels.

The paper is organized such that, we first discuss briefly about various data fusion techniques in remote sensing domain, satellite data and inferences, then the Kalman equations, finally concluding the image-quality enhancement of fused data in results and conclusion section.

2. Related work

Development of various data fusion techniques is an active research area in Geoscience and remote sensing applications. Here we have brief description of various techniques. Typically, the algorithms for remote sensing image employing pixel-level fusion can be divided into three general categories, component substitution (CS) fusion technique [4-7], modulation-based fusion technique [8-10] and multi-resolution analysis (MRA) based fusion technique [11-12].

The typical algorithms of component substitution fusion technique are intensity hue saturation (IHS) transform fusion algorithm [5-6, 13]. This algorithm is suitable when exactly three multispectral (MS) bands are concerned since the IHS transform is defined for three components only. When more than three bands are available, Tu, *et al.*, [14] presented a generalized IHS (GIHS) transform by including the response of the near-infrared (NIR) band into the intensity component. In order to overcome color distortion problem in IHS and the wavelet fusion technique Zhang and Hong [15] presented a new fusion approach that integrates the advantages of both the IHS and the wavelet techniques to reduce the color distortion of IKONOS and QuickBird fusion results. Visual and statistical analyses demonstrated that the new IHS and wavelet integrated fusion approach does improve the fusion quality of the IKONOS and QuickBird images compared to the original IHS technique and the wavelet technique.

Garzelli and Nencin [16] proposed Generalized Intensity-Hue-Saturation-Genetic algorithm (GIHS-GA) based on CS strategy and genetic algorithm. The weights of the MS bands in synthesizing the intensity component and the injection gains are achieved by minimizing a global distortion metrics by means of a GA.

GIHS with Tradeoff Parameter (GIHS-TP) [17] is a CS-based method that trades off the performances of GIHS in terms of spectral distortion and spatial enhancement. Gonzáles Audícana and Otazu [18-19] presented a low computational-cost method to fuse IKONOS images using the spectral response function of its sensors. Andreja and Krisˇtof [20] found that for preserving spectral characteristics, a high level of similarity between the panchromatic image and the respective multispectral intensity is needed. In order to preserve spectral and spatial resolution, spectral sensitivity of multispectral and panchromatic data was performed, and digital values in individual bands were modified before fusion. Aiazzi, *et al.*, [7] adopted multivariate regression to create the synthetic low-resolution-intensity images which is used in the Gram-Schmidt transform. The proposed enhanced strategy is effective in improving the quality of the images than ordinary GS technique.

Ling and Ehlers, *et al.*, [21] presented a method which combines a standard IHS transform with FFT filtering of both the panchromatic image and the intensity component of the original multispectral image. Other common used CS-based method, PCA transform [5-6], assumes that the first principal component (PC) of high variance is an ideal choice for replacing or injecting it with high spatial details from the high-resolution histogram-matched PAN image. Shah, *et al.*, [22] used the adaptive PCA to reduce the spectral distortion in the fusion scheme combining adaptive PCA approach and contourlets. Another CS technique reported in the literature is Gram–Schmidt (GS) spectral sharpening [23], which is widely used since it has been implemented in the Environment for Visualizing Images (ENVI) program package.

Li and He [24] proposed a new pan sharpening approach that integrates the advantage of both the Induction and correspondence analysis techniques to reduce the color distortion of IKONOS and Quick Bird fusion results. In order to solve the color distortion problem in the fusion process, the new approach takes two steps. First, using Induction to upscale the MS images to overcome the miss-registration problem caused by cubic interpolation; second, injecting the spatial details from PAN image into MS images by correspondence analysis to better preserve the spectral information of the MS images.

The modulation-based fusion technique utilizes the concept that the spatial details are modulated into the multispectral images by multiplying the multispectral images by the ratio of the panchromatic image to the synthetic image, which is a lower resolution version of the panchromatic image generally. Typical modulation based fusion algorithms include High-pass filtering (HPF) method by Chavez [6] Synthetic Variable Ratio (SVR) merging method by Zhang [9], Brovey transform fusion algorithm by Vrabel [25], Smoothing Filter Based Intensity Modulation (SFIM) fusion algorithm by Liu [8] and optimized the high pass filter addition technique By Gangkofner, *et al.*, [10].

Multi resolution analysis (MRA) based fusion techniques adopt multi-scale decomposition methods such as multi-scale wavelet and Laplacian pyramid to decompose multi-spectral and panchromatic images with different levels, and then derive spatial details that are imported into finer scales of the multi-spectral images in the light of the relationship between the panchromatic and multi-spectral images in coarser scales, resulting in enhancement of spatial details [11-12, 26].

Ranchin, *et al.*, [27] presented the method for improving spatial resolution by structure injection, the concept was based on the assumption that the missing information is linked to the high frequencies of the datasets to be fused. Some fusion techniques jointly using component substitution with multi-scale analysis were developed, such as the algorithms combing wavelet transform and IHS transform [15, 28, 29] or PCA transform [22]. These hybrid schemes used wavelets to extract the detail information from one image and standard image transformations to inject it into another image, or propose improvements in the method of injecting information [30].

Otazu, *et al.*, [19] introduced concept of sensors spectral response and ground spectral features into fusion technology based on MRA. Aanæs, *et al.*, [31] utilized the regularization method to optimize the fusion results to satisfy the higher resolution multispectral image model. Yang, *et al.*, [32] generalized this idea and proposed a new model quantifying the mathematical relationship between the fused higher multispectral images and the original multispectral image, the spatial details being extracted from the high-resolution panchromatic image, and the adopted fusion strategies.

A detailed literature could be found in special issues and recent review papers published pertaining to various algorithms [33-37].

3. Satellite Data and Inferences

Input data is an image collected by Ozone Monitoring Instrument (OMI) on NASA's Aura satellite [38]. The sensors are specialized developed to tracks global ozone changes and monitors aerosols in the atmosphere. Figure 1 and Figure 2 shows input and output images.

Out-of-control fires burning on the eastern shore of Sumatra (center of image) created an air quality emergency for bordering Malaysia in early August 2005 as smoke shrouded few parts of the countryside. The smoke hung densely over Malaysia's busy capital, Kuala Lumpur. Red-colored areas give you an idea about where smoke was thickest. The densest smoke hangs over the Strait of Malacca, between Sumatra and mainland Malaysia to the northeast. Winds in this region regularly blow from the west, diffusing smoke from burning peat swamp forest in coastal Sumatra toward the east. The thickness of the smoke tapers off to mostly green and blue values between mainland Malaysia and the island of Borneo, farther east.

A less concentrated smoke plume is located on the west coast of Borneo, coming from a much smaller assortment of fires. The smoke contains many substances like water vapor, carbon dioxide, carbon monoxide, and particulate matter. OMI measures smoke by tracking black carbon particles, or soot, that absorb ultraviolet (UV) radiation, the wavelengths of sunlight that cause sunburns. By measuring the amount of UV radiation, OMI provides estimates of the amount of black carbon aerosol in the smoke layer. This method of detecting aerosols based on their interaction with UV rather than visible (rainbow) light allows OMI to measure absorption by black carbon in smoke even if the smoke is mixed with or floating on top of the clouds. Thus to sum up, the image under study depicts 'Air Quality Emergency in Malaysia".

Proper inferences on the satellite data is an active research area in global warming domain. The net effect of aerosols on Earth's energy budget and global climate change can be studied by measuring how much radiation can be absorbed by the aerosols.

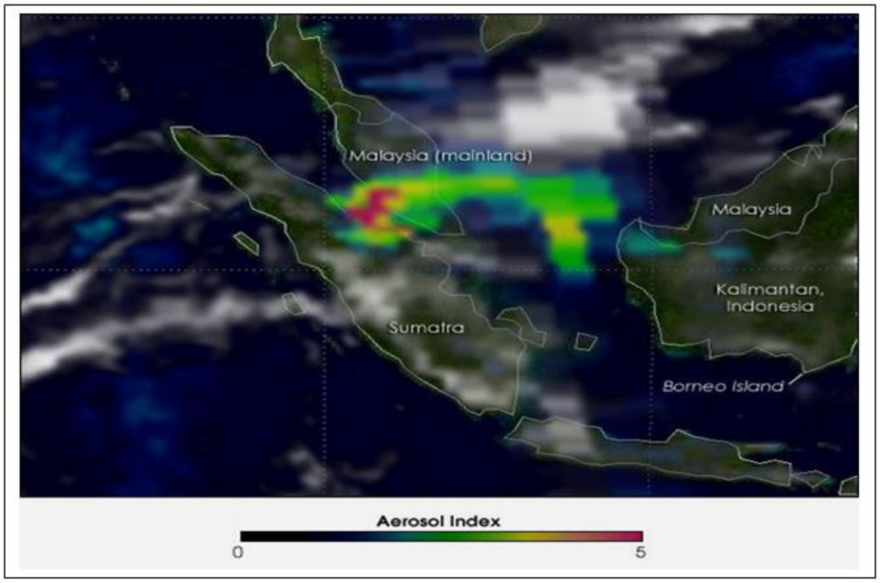

Figure 1. Input Image
(The image of Malaysia captured by the OMI on NASA's Aura satellite [38])

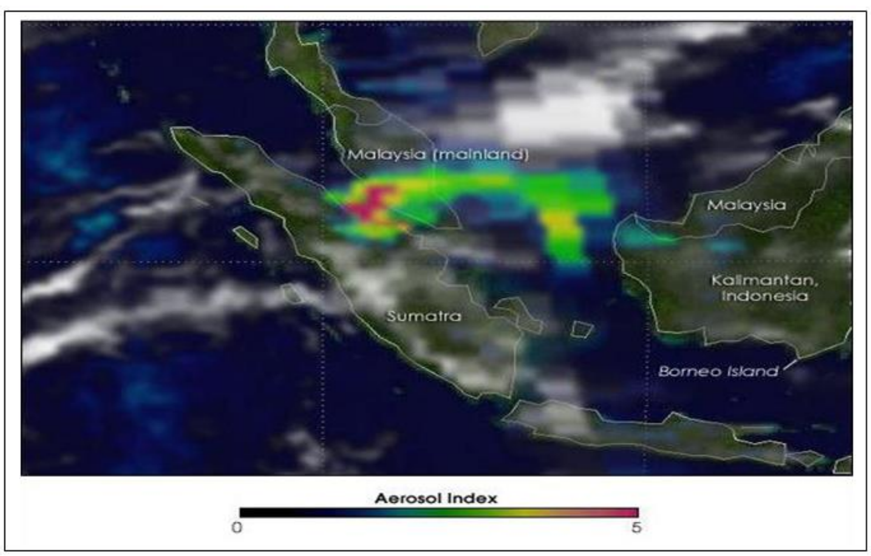

Figure 2. Output image (Kalman filtered-fused image)

4. Kalman Equations

The representation of an image in a Kalman filter can either be or block-wise or pixel-wise, here we have considered the latter approach. The image model is as follows. Let x_k represent a particular pixel found in frame k (taken at time k) of the image .Then, each pixel represents a time series in frame k.

The Kalman equations are as follows:

The ideal noise-free pixel value is given by S_k , which is assumed to be a first order Adaptive Recursive model. This model is generally used to study the behavior of pixels in video signals [39].

The process model is

$$s_{k+1} = as_k + n_k , \qquad (1)$$

where a is a constant that depends on the signal statistics and n_k is the process noise, which is assumed to be white Gaussian with zero mean and variance σ^2_n . Assuming that noise is Gaussian simplifies the design. On the other hand, it will be desirable to construct the class of filters in such a way as to be extensible to different noise sources. Thus, the measured signal is given by

$$x_k = s_k + v_k \qquad (2)$$

where v_k is the independent additive zero mean Gaussian white noise with variance of σ^2_v .

If the noise and signal are wide-sense stationary random processes that are fully determined by their second-order statistics, then the Kalman filter is essentially a Weiner Filter.

The Kalman filter output is represented by y_k, which is the estimate of the signal at time k. The variance of the estimation error variance is defined by

$$\sigma^2_k = E [(y_k - s_k)^2] \qquad (3)$$

The Kalman filter gain is K_k.

For the single pixel case, the Kalman filtering algorithm is given by the following algorithm.

We consider y-1 =0 and σ^2-1 = σ^2_v ,

$$K_k = \frac{a^2\sigma^2(k-1) + \sigma_n^2}{a^2\sigma^2(k-1) + \sigma_n^2 + \sigma_v^2} \qquad (4)$$

$$y_k = K_k x_k + a[1- K_k] yk\text{-}1, \qquad (5)$$

$$\sigma^2_k = a^2 [1- K_k] \sigma^2_{k-1} + \sigma^2_n. \qquad (6)$$

This algorithm is applied to each pixel, and each time instant. The estimated pixel value, y_k is output for each iteration, k to provide the filtered image output for display or image analysis purposes. The updated Kalman filter gain K_k and updated noise estimation, $\sigma^2_{k,}$ are also output at each iteration. As before, a is a constant that depends on the signal statistics.

The Kalman filter will output the updated, filtered estimates of the pixels from each of the cameras. In addition, the covariance of the errors in the state estimates at each time k provides information as to the reliability of the estimates. If the state covariance matrix is not diagonal, then there exists a transformation of the states so that the covariance of the new states is diagonal. That transformation is given by the matrix whose columns are the eigenvectors of Pk(+), Let t_i be the ith eigenvector of Pk(+). Then,

$$Pk(+)\ t\ k,i = \lambda i\ tk,i \quad (7)$$

and

$$\hat{\hat{x}}_k(+) = T_k \hat{x}_k(+) \quad (8)$$

where Tk is the matrix whose columns are the orthonormal eigenvectors.

Since new states are statistically independent of each other with known variances given the eigenvalue associated with the corresponding eigenvector, a weighted average pixel can computed. The weights represent the fraction of the total variance associated with each element of $\hat{\hat{x}}_k(+)$ and are given by

$$\omega_i = \frac{1/\lambda_i}{\sum_i 1/\lambda_i}. \quad (9)$$

The optimal estimate of the pixel value is

$$\bar{\bar{x}}_k(+) = \sum_i \hat{\hat{x}}_{k,i}(+)\omega_i \quad (10)$$

Thus, the output image is formed with fusion of optimal estimates of pixel values.

5. Results and Discussion

The input satellite image is subjected to proposed algorithm. The output or fused image however, often needs to be correlated with the original image, in order to ensure that the resulting image is rendering better quality. Aside from the visual examination, which is mandatory, image quality indices such as correlation coefficient, entropy, universal image quality index, anisotropy, and Von Mises (VM) distribution and many others are very useful, when deciding which fused image is the most satisfactory [40].

We have selected few image quality indices to compare and contrast original and fused images.

Although the comparison results are not so enormously exciting but are convincing and satisfactory, please refer Tables 1 to 4.

1) ***Image Entropy (E):*** This index reflects the amount of information included in a certain image. Entropy requires histogram analysis: p is the percentage of the pixels, whose value falls into a certain bin class, while bc, is the total number of bin classes. It is given by :

$$E = -\sum_{i=1}^{bc} p * log_2(p)$$

2) ***Correlation Coefficient (CC):*** It characterizes the correlation between the original and the processed image. It is considered as a reliable index and is commonly used. It has a dynamic range of [-1 1]. Value zero, indicates absolutely no correlation between the x data

and y data, while value 1, indicates that x = y. Value -1, means that x is the exact opposite of y, or x = -y.

$$CC = \frac{\sigma_{xy}}{\sigma_x \sigma_y}$$

3) ***Universal image quality index (Q):*** It describes the quality of the processed image. It is a stout index, as it uses x, y means and standard deviations, to produce the result. Like correlation coefficient, it has a dynamic range of [-1 1] with the same interpretations in values.

$$Q = \frac{4\,\sigma_{xy}\,\overline{x}\,\overline{y}}{(\sigma_x{}^2 + \sigma_y{}^2)[\overline{x}^2 + \overline{y}^2]}$$

4) ***Anisotropy:*** Quality and entropy are fairly related issues. If the source is a given image, the obstacle for the entropy to be considered a quality index is that noise cannot be distinguished from information, noise being a kind of information itself. From a human observer point of view, objects constitute the areas of interest in a picture, and humans with good eye correction are easily capable of distinguishing the sharpest objects. Noise or blurring is easily identifiable by the visual system. Analytically, entropy increases with sharpness but, in general, there is not a fair correlation when images are noisy. Hence, entropy by itself is not a good indicator of image quality. To overcome this problem, we have used measure of anisotropy also as a measure of image quality.

Anisotropy is certainly one of the properties of natural images and is related to its directional dependency. Image anisotropy is sensitive to noise and blur parameters. Directional entropy can be achieved by means of the Rényi entropy. Differences in the directional entropy give the figure of anisotropy, which is used to measure image quality [41].

$$R_\alpha[n] = -\frac{1}{2}\log_2\left(\sum_{k=1}^{N} \check{P}_n^{\alpha}[k]\right)$$

Where R = Rényi entropy measure, P= probability density function, here n and k represent the spatial and frequency variables, respectively. In addition, $\alpha \geq 2$ are values recommended for space–frequency distribution measures [41].

5) ***Von Mises (VM) distribution:*** The von Mises (VM) distribution belongs to probability theory and is used to handle directional statistics for continuous probability distribution on a circular basis. It appears, in many respects, analogous to the normal distributions for a scalar variable. This distribution has also been applied to diverse applications in many fields and has become an important tool in the statistical theory of directional data [42]. The difference in distribution values for input and output images are shown in Figure 3 and 4.

The standard form of the Von Mises probability density function is:

$$f(x|\mu,\kappa) = \frac{e^{\kappa \cos(x-\mu)}}{2\pi I_0(\kappa)}$$

where $I_0(x)$ is the modified Bessel function of order zero.

The parameters μ and 1/κ are analogous to μ and σ2 (the mean and variance) in the normal distribution. μ is a measure of location (the distribution is clustered around μ), and κ is a measure of concentration (a reciprocal measure of dispersion, so 1/κ is analogous to σ2). If κ is zero, the distribution is uniform, and for small κ, it is close to uniform. If κ is large, the distribution becomes very concentrated about the angle μ with κ being a measure of the concentration. In fact, as κ increases, the distribution approaches a normal distribution in x with mean μ and variance 1/κ.

Table 1.

Image Entropy (E)		
Band	Input Image	Output Image (Kalman filtered)
1	6.4219	6.5602
2	6.6255	6.7290
3	6.5638	6.6798
Average	6.5371	6.6563
Total	6.7255	6.8415

Table 2.

Correlation Coefficient (CC)		
Band	Input Image	Output Image (Kalman filtered)
1	0.95199	1
2	0.95207	1
3	0.93865	1
Average	0.94757	1

Table 3.

Universal image quality index (Q)		
Band	Input Image	Output Image (Kalman filtered)
1	0.95198	1
2	0.95207	1
3	0.93864	1
Average	0.94756	1

Table 4.

Anisotropy		
Channel	Input Image	Output Image (Kalman filtered)
1	0.0084925	0.0088653
2	0.0074219	0.0078563
3	0.0072386	0.0074903
Average	0.0077	0.0081

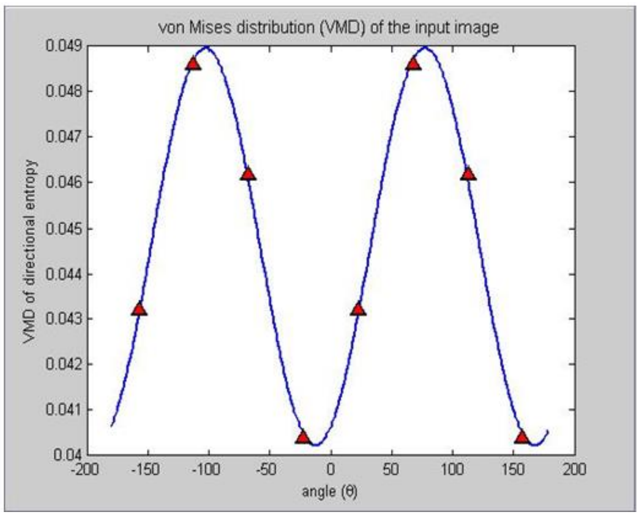

Figure 3. Von Mises distribution for input image

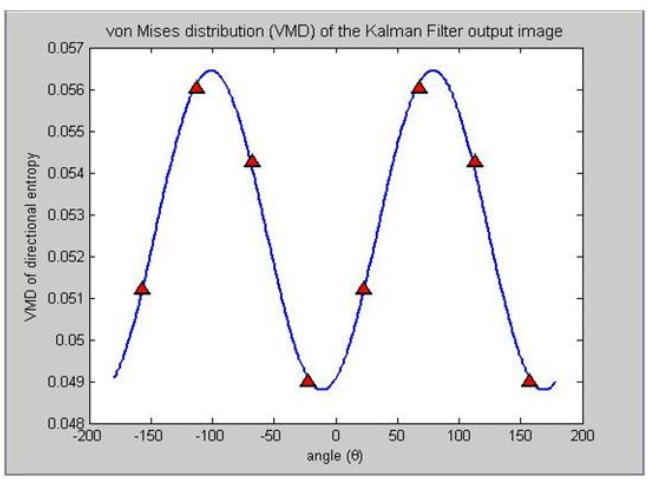

Figure 4. Von Mises distribution for output image

6. Conclusion

Image quality is understood as the subjective impression of how well the image content is rendered or reproduced for better interpretation and inferences. Image fusion is one of the significant tools to improve the image quality. The paper presents satellite image fusion at pixel-level. The output image is formed with fusion of optimal estimates of pixel values. Image quality assessment is done by various quality metrics and it is tried to affirm the potential of proposed Kalman filter implementation in multisensor satellite data fusion.

References

[1] C. Pohl and J. L. V. Genderen, "Multisensor image fusion in remote sensing: concepts, methods and applications", Int. J. Remote sensing, vol. 19, no. 5, **(1998)**, pp. 823-854.
[2] J. Biemond, J. Riesek and Gerbrands, "A fast Kalman filter for images degraded by both blur and noise", IEEE Trans. Acoust., Speech, Signal Process, vol. 31, no. 5, **(1983)**, pp. 1248–56.
[3] R. E. Kalman, "A New Approach to Linear Filtering and Prediction Problems", Transaction of the ASME—Journal of Basic Engineering, **(1960)**, pp. 35-45.
[4] A. H. J. M. Pellemans, R. W. L. Jordans and R. Allewijn, "Merge Multispectral and Panchromatic SPOT Images with respect to the Radiometric Properties of Sensor", Photogramm. Eng. Remote Sens., vol. 59, no. 1, **(1993)**, pp. 81-87.
[5] V. K. Shettigara, "A generalized component substitution technique for spatial enhancement of multispectral images using a higher resolution data set", Photogramm. Eng. Remote Sens., vol. 58, **(1992)**, pp. 561–567.
[6] S. Chavez, C. Sides and A. Anderson, "Comparison of three different methods to merge multiresolution and multispectral data: Landsat TM and SPOT panchromatic", Photogramm. Eng. Remote Sens., vol. 57, **(1991)**, pp. 295-303.
[7] B. Aiazzi, S. Baronti and M. Selva, "Improving Component Substitution Pansharpening Through Multivariate Regression of MS +Pan Data", IEEE Transactions on Geoscience and Remote Sensing, vol. 45, no. 10, **(2007)**, pp. 3230–3239.
[8] J. G. Liu, "Smoothing Filter-based Intensity Modulation: a spectral preserve image fusion technique for improving spatial details", International Journal of Remote Sensing, vol. 21, **(2000)**, pp. 3461-3472.
[9] Y. Zhang, "A new merging method and its spectral and spatial effects", International Journal of Remote Sensing, vol. 20, no. 10, **(1999)**, pp. 2003-2014.
[10] U. G. Gangkofner, P. S. Pradhan and D. W. Holcomb, "Optimizing the High-pass filter addition technique for image fusion", Photogrammetric Engineering and Remote Sensing, vol. 74, no. 9, **(2008)**, pp. 1107-1118.
[11] B. Aiazzi, L. Alparone, S. Baronti and A. Garzelli, "Context-driven fusion of high spatial and spectral resolution images based on oversampled multiresolution analysis", IEEE Transactions on Geoscience and Remote Sensing, vol. 40, **(2002)**, pp. 2300-2312.
[12] K. Amolins, Y. Zhang and P. Dare, "Wavelet based image fusion techniques — An introduction, review and comparison", ISPRS Journal of Photogrammetry & Remote Sensing, vol. 62, **(2007)**, pp. 249–263.
[13] J. W. Carper, T. M. Lillesand and R. W. Kiefer, "The use of intensity–hue–saturation transformations for merging SPOT panchromatic and multispectral image data", Photogramm. Eng. Remote Sens., vol. 56, **(1990)**, pp. 459–467.
[14] T. -M. Tu, P. S. Huang, C. -L. Hung and C. -P. Chang, "A fast intensityhue-saturation fusion technique with spectral adjustment for IKONOS imagery", IEEE Geosci. Remote Sens. Lett., vol. 1, no. 4, **(2004)**, pp. 309–312.
[15] Y. Zhang and G. Hong, "An IHS and wavelet integrated approach to improve pan-sharpening visual quality of natural color IKONOS and QuickBird images", Information Fusion, vol. 6, Issue 3, **(2005)** September, pp. 225–234.
[16] A. Garzelli and F. Nencini, "Fusion of panchromatic and multispectral images by genetic algorithms", Proceedings of IEEE Geoscience Remote Sensing Symposium, **(2006)**, pp. 3810–3813.
[17] M. Choi, "A New Intensity-Hue-Saturation Fusion Approach to Image Fusion with a Tradeoff Parameter", IEEE Transactions on Geoscience and Remote Sensing, vol. 44, no. 6, **(2006)**, pp. 1672-1682.
[18] M. Gonzáles Audícana, X. Otazu, O. Fors and J. A. Alvarez-Mozos, "A low computational-cost method to fuse IKONOS images using the spectral response function of its sensors", IEEE Trans. Geosci. Remote Sens., vol. 44, no. 6, **(2006)**, pp. 1683–1691.

[19] X. Otazu, M. González-Audícana and O. Fors, "Introduction of Sensor Spectral Response into Image Fusion Methods: Application to Wavelet-Based Methods, IEEE Transactions on Geoscience and Remote Sensing, vol. 43, no. 10, **(2005)**, pp. 2376-2385.
[20] S. Andreja and O. Krisˇtof, "High-resolution Image Fusion: Methods to Preserve Spectral and Spatial Resolution", Photogramm. Eng. Remote Sens., vol. 72, no. 5, **(2006)**, pp. 565-572.
[21] Y. R. Ling, M. Ehlers, E. L. Usery and M. Madden, "FFT-enhanced IHS transform method for fusing high-resolution satellite images", ISPRS J. Photogramm. Remote Sens., vol. 61, **(2007)**, pp. 381–392.
[22] V. P. Shah, N. H. Younan and R. L. King, "An efficient pan-sharpening method via a combined adaptive PCA approach and contourlets", IEEE Trans. Geosci. Remote Sens., vol. 46, no. 5, **(2008)**, pp. 1323–1335.
[23] C. A. Laben and B. V. Brower, "Process for enhancing the spatial resolution of multispectral imagery using Pan sharpening", U.S. Patent 6 011 875, Tech. Rep, Eastman Kodak Company, **(2000)**.
[24] X. Li and M. He, "A Novel Pan sharpening Algorithm for IKONOS and Quick Bird Images", IEEE TRANSACTIONS on Geoscience and Remote sensing, **(2009)**.
[25] J. Vrabel, "Multispectral imagery advanced band-sharpening study", Photogramm. Eng. Remote Sens., vol. 66, **(2000)**, pp. 73- 79.
[26] J. N´u˜nez, X. Otazu, O. Fors, A. Prades, V. c Pal`a and R.Arbiol, "Multi resolution-Based Image Fusion with Additive Wavelet Decomposition", IEEE Transactions on Geoscience and Remote Sensing, vol. 37, **(1999)**, pp. 1204 – 1211.
[27] T. Ranchin, B. Aiazzi, L. Alparone, S. Baronti and L. Wald, "Image fusion—the ARSIS concept and some successful implementation schemes", ISPRS Journal of Photogrammetry and Remote Sensing, vol. 58, **(2003)**, pp. 4-18.
[28] M. González-Audícana, J. L. Saleta and R. G. Catalán, "Fusion of Multispectral and Panchromatic Images Using Improved IHS and PCA Mergers Based on Wavelet Decomposition", IEEE Transactions on Geoscience and Remote Sensing, vol. 42, no. 6, **(2004)**, pp. 1291-1299.
[29] Y. Chibani and A. Houacine, "The joint use of IHS transform and redundant wavelet decomposition for fusing multispectral and panchromatic images", International Journal of Remote Sensing, vol. 23, no. 18, **(2002)**, pp. 3821-3833.
[30] A. Garzelli and F. Nencini, "Interband structure modeling for Pan-sharpening of very high-resolution multispectral images", Information Fusion, vol. 6, **(2005)**, pp. 213-224.
[31] H. Aanæs, J. R. Sveinsson, A. A. Nielsen, T. Bøvith and J. A. Benediktsson, "Model-Based Satellite Image Fusion", IEEE Transactions on Geoscience and Remote Sensing, vol. 46, no. 5, **(2008)**, pp.1336-1346.
[32] J. H. Yang, J. X. Zhang and H. T. Li, "Generalized Model for Remotely Sensed DataPixel-Level Fusion and Its implementation technology", Journal of Image and Graphics (Chinese), vol. 14, no. 4, **(2009)**, pp. 604–614.
[33] P. Gamba and J. Chanussot, "Guest Editorial Foreword to the Special Issue on Data Fusion", IEEE Transactions on Geoscience and Remote Sensing, vol. 46, no. 5, (**2008)**, pp.1283-1288.
[34] L. Alparone, L. Wald, J. Chanussot, C. Thomas, P. Gamba and L. M. Bruce, "Comparison of Pansharpening Algorithms: Outcome of the 2006 GRS-S Data-Fusion Contest", IEEE Transactions on Geoscience and Remote Sensing, vol. 45, no. 10, **(2007)**, pp. 3012-3021.
[35] G. Asha and A. Philip, "Pixel Level Satellite Image Fusion Using component Substitution Partial Replacement", International Journal of Computer Engineering Science, vol. 1, Issue 3, **(2011)** December, pp. 7-16.
[36] Y. Jinghui, Z. Jixian, L. Haitao, S. Yushan and P. Pengxian, "Pixel level fusion methods for remote sensing images: A current review, International Society for Photogrammetry and Remote Sensing (ISPRS), vol. XXXVIII, Part 7B, **(2010)** July 5–7, Vienna, Austria.
[37] D. Jiang, D. Zhuang, Y. Huang and J. Fu, "Survey of Multispectral Image Fusion Techniques in Remote Sensing Applications in book, Image Fusion and Its Applications, Edited Yufeng Zheng, Alcorn State University, USA, **(2011)**.
[38] http://visibleearth.nasa.gov/view.php?id=15336.
[39] M. Piovoso and P. A. Laplante, "Kalman filter recipes for real-time image processing", Real-Time Imaging, vol. 9, **(2003)**, pp. 433–439.
[40] A. D. Vaiopoulos, "Developing Matlab scripts for image analysis and quality assessment", Proceedings of SPIE 8181, Earth Resources and Environmental Remote Sensing/GIS Applications II, **(2011)**, Prague, Czech Republic.
[41] S. Gabarda and G. Cristobal, "Blind image quality assessment through anisotropy", J. Opt. Soc. Am., vol. 24, no. 12, **(2007)**, pp. 1-10.
[42] S. Gabarda and G. Cristobal, "No-reference image quality assessment through the von Mises distribution", J. Opt. Soc. Am., vol. 29, no. 10, **(2012)**, pp. 2058-2066.

Authors

S. A. Quadri is associated with Collaborative Micro-electronic Design Excellence Centre (CEDEC). His research domain includes multisensor data fusion in various engineering applications and neural networks.

Professor Othman bin Sidek an esteemed Malaysian scientist graduated as Bachelor in Applied Science in Electronics (Honors) from Universiti Sains Malaysia and went on to earn a Master of Science Degree in Communication engineering from UMIST, UK, as well as a PhD in Information Systems Engineering from Bradford University, UK. He is also the Founder and Director of the Collaborative Micro-electronic Design Excellence Centre (CEDEC), an approved centre at Universiti Sains Malaysia by the Malaysian Ministry of Finance in 2005 out of his own initiative. His current research areas mainly focus on Micro-Electro Mechanical Systems (MEMS) and Wireless Sensor Network, Embedded System/SOC and VLSI/ASIC Design. All these are the focused areas of CEDEC.